

We are IntechOpen, the world's leading publisher of Open Access books Built by scientists, for scientists

6,900

Open access books available

186,000

International authors and editors

200M

Downloads

Our authors are among the

154

Countries delivered to

TOP 1%

most cited scientists

12.2%

Contributors from top 500 universities



WEB OF SCIENCE™

Selection of our books indexed in the Book Citation Index
in Web of Science™ Core Collection (BKCI)

Interested in publishing with us?
Contact book.department@intechopen.com

Numbers displayed above are based on latest data collected.
For more information visit www.intechopen.com



Nanodesign and Simulation Toward Nanoelectronic Devices

Sang Uck Lee¹ and Yoshiyuki Kawazoe²

¹Corporate R&D / LG Chem. Research Park

²Institute for Materials Research, Tohoku University

¹Korea

²Japan

1. Introduction

The low-dimensional allotropes of carbon have drawn much attention in a multitude of fields owing to their outstanding fundamental properties and potential for applications. Interest in such systems has branched out from carbon fullerenes and carbon nanotubes (CNTs) toward other novel carbon nanomaterials such as graphitic onions, cones, nanohorns, nanohelices, nanobarrels, and graphene. All of these unique carbon nanomaterials show promising capabilities for applications in electronic devices.

Especially, CNT has the potential to make the process of development of electronics comprehensible to us as well as conquering many of the size limitations of the circuits with possible applications in integrated circuits and energy conservation. It is believed that CNT-electronics shares the potential, together with Biotechnology and Artificial Intelligence to improve current devices. Such advances can then be used to solve problems not possible in present. Conductive and high-strength composites; energy conversion and energy storage devices; sensors; field emission displays and radiation sources; hydrogen storage media; and nanometer-sized semiconductor devices, probes, and interconnects are some of the many potential applications based on carbon nanotubes. Some of these applications are now realized in products. Others are demonstrated in early to advanced devices.

In the field of electronics, experiments over the past several years have given researchers hope that wires and functional devices tens of nanometres or smaller in size could be made from such low-dimensional materials and incorporated into electronic circuits that work far faster and on much less power than those existing today. In the long term, the most valuable applications will take further advantage of the unique electronic properties of low-dimensional materials. Surrounded by such anticipation, the advancement of techniques for characterizing and manipulating of individual molecules and the availability of first-principles methods to describe electron tunneling through atomic chains or single molecules have facilitated the development of a variety of electronic devices, attesting to the potential utility of these molecules in nanoelectronic device architectures.

Few possible applications of CNT in electronics are discussed below:

Carbon nanotube field-effect transistors (CN-FETs): CNT is one of the candidates for a quantum wire for the molecular-FET. Multi-channel carbon nanotube field-effect transistors (CNFETs) have been realized by depositing a large number of CNTs onto a metallic back gate. This work clearly demonstrates that CN-FETs are promising components for high-

frequency (HF) applications. Recently, several works have been reported on the CNTs for FETs and CNT-logic applications.

Transistors: IBM has made CN-FET resembling to conventional MOSFET having conduction channel beneath the gate electrodes separated by a thin dielectric. The top gate devices exhibited excellent electrical characteristics, including steep sub-threshold slope and high transconductance at low voltages by reducing the gate-to-channel separation. Furthermore, the IBM scientists were able to fabricate both hole (p-type) and electron (n-type) transistors. The top-gate design allows independent gating of each transistor, making it possible to generate CMOS (complementary metaloxide semiconductor) circuits that have a simpler design and consume less power. The nanotube devices in this case outperformed the prototype silicon transistor.

Logic circuits: The first inter-molecular logic circuit has been created by IBM. The circuit is a voltage inverter made by using two nanotube field-effect transistors.

Diodes: A nanotube formed by joining nanotubes of two different diameters end to end can act as a diode, suggesting the possibility of constructing electronic computer circuits entirely out of nanotubes. A “p-n junction” is simulated along the single-walled carbon nanotube channel using two separate gates close to the source and drain of the CNTFET, respectively. The Schottky barrier field-effect transistor mechanism-based calculations of the current-voltage characteristics of the double-gated CNTFET show a good rectification performance of the p-n junction.

As like the applications, CNTs have been evinced as the material of future which will assist in extending the Moore’s law, which says that number of transistors per integrated circuit doubles every 18 months, and it has been the guiding principle for the semiconductor industry for over 30 years. The prime driving force in nanoelectronic industry is due to the continual miniaturization of electronic devices.

However, it will be progressively difficult to continue downscaling at this rate, as quantum tunneling, interconnect delays, gate oxide reliability, and excessive power dissipation, among other factors, start hampering the performance of such devices. While some of these issues can, in principle, be handled by improving device design, packaging, processing, and channel mobilities, the rapidly increasing cost of fabrication motivates exploration of entirely new paradigms, such as novel architectures and new channel materials. One promising direction involves replacing the “top-down” lithographic approach with a “bottom-up” synthetic chemical approach of assembling nanodevices and circuits directly from their molecular constituents. Molecules are naturally small, and their abilities of selective recognition and binding can lead to cheap fabrication using self-assembly. In addition, they offer tenability through synthetic chemistry and control of their transport properties due to their conformational flexibility.

In the case of CNTs, significant progress has been reported regarding synthesis, functionalization, and control of the electronic properties. Insertion into and doping of CNTs are steps toward nanotube functionalization, possibly opening pathways to the creation of nanoelectronic devices, to the synthesis of heteronanotubes, and to the application of CNTs in many fields of science. However, their use as building blocks for nanoelectronic devices has not yet been fully realized due to lack of control of the reactivity of the outer CNT walls and of the basic electronic structure.

Therefore, for electronics applications, it is very desirable to modify the electronic structure of CNT to obtain a metallic or a p- and n-type semiconducting behavior. Many attempts at

this direction have been reported. The energy gap can be adjusted by changing the chemical composition. For instance, boron and nitrogen atoms are among the atoms most conveniently used as dopants of CNTs, since they have atomic sizes similar to that of carbon, a property that provides them with a strong probability of entering into the carbonaceous lattice. In addition, it has also been experimentally and theoretically reported that the doping of CNTs with nitrogen atoms tailors the electronic structure of the nanotube by introducing donor states near the Fermi level with additionally localized nonbonding states of lone pair electrons, which brings about an enhancement of electron conduction of semiconducting CNTs at low temperature. Even though it is possible to functionalize and control the electronic properties of CNT through chemical doping, fine tuning of doping concentration remains very difficult. Another method for CNT electronic structure engineering is non-covalent modification, i.e. encapsulation. Recently, air-stable amphoteric doping on CNTs has been realized by encapsulating organic molecules inside CNTs and it has been found that the carrier type and concentration in CNT can easily be controlled by tuning the electron affinity (EA) and ionization potential (IP) of the encapsulated molecules. Compared to previously investigated metal atoms or fullerenes encapsulated CNTs, there are many advantages in using an organic molecule encapsulation. Organic molecules are typically stable in air, simple to synthesize, and abundant. They have already been used to adjust the CNT band structure.

In this chapter, I will show how we can design nanoelectronic component embodied with interesting device characteristics, especially rectifying diodes. Simple strategy for designing nanoelectronic diodes is creating CNT heterojunction and controlling their electronic structure. In view of incorporating CNTs into real operational nanodevices, CNT-based intramolecular junctions were proposed early on. As mentioned before, a diode electronic component has been realized by joining nanotubes of two different diameters end to end. Both theoretical and experimental studies of such nanojunctions are full of promise. The junctions can be designed through various conceivable linkages within one-dimensional morphologies, such as a direct covalent bond, organic or metallic linkages, and even spacing. Such formation of one-dimensional heterojunctions has led to materials with unique properties and multiple functionalities not realized in single-component structures that are useful for a wide range of applications.

Especially, I will introduce how we can design and simulate conventional three types of diodes, Zener-, Schottky-, and Esaki-type diodes. I will introduce that the CNT junctions with chemical or physical doping, and organic linkages open the door to the design nanoelectronic components embodied with unique electron transport characteristics as nanoelectronic devices. The designed nanoelectronic components will give an insight into the design and implementation of various electronic logic functions based on CNTs for applications in the field of nanoelectronics.

2. Theoretical methodology

Remarkable progress in the molecular(nano) electronics has been made in the last few years, as researchers have developed ways of growing, addressing, imaging, manipulating, and measuring small groups of molecules connecting metal leads. Several prototype devices such as conducting wires, insulating linkages, rectifiers, switches, and transistors have been demonstrated. In parallel, there has been significant theoretical activity toward developing the description of nonequilibrium transport through molecules.

Transport through a molecule under bias is essentially a nonequilibrium, quantum kinetic problem. Contacting a molecule with two leads effectively “opens up” the system, replacing the discrete molecular energy levels with a continuous density of states and establishing a common electrochemical potential and a band lineup between the contacts and the molecule. Under bias, the two contact electrochemical potentials split, and the molecule, in its bid to establish equilibrium with both contacts, is driven strongly out of equilibrium. Current flow thus requires a formal treatment of nonequilibrium transport, through a suitable wave function (scattering theory) or Green’s function technique. The Keldysh-Kadanoff-Baym nonequilibrium Green’s function (NEGF) formalism gives us a rigorous theoretical basis for describing quantum transport through such a system at an atomistic level.

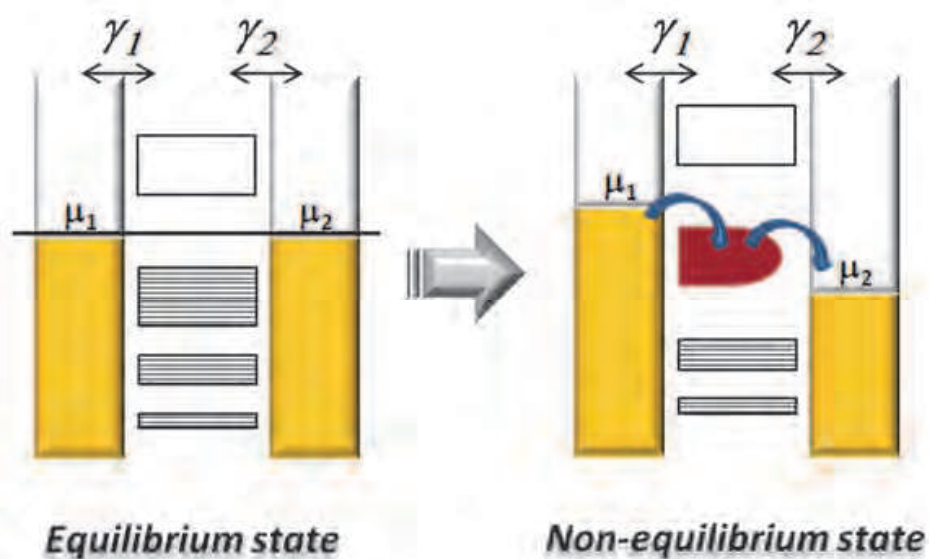


Fig. 1. Electron flow under applied bias.

This approach has been proven to be a powerful tool for studying electron-transport phenomena in nanodevices, and it provides a link between electron transport, first-principles electronic structure theory, and qualitative molecular orbital theory.

A typical simulation procedure consists of self-consistently coupling an electronic structure calculation with a suitable transport solver. Transport involves a nonequilibrium, open-boundary problem. We formally partition this problem into an active device and semi-infinite contacts that add or remove charges from it. The device energy levels and electrostatics are described by a Hamiltonian and a self-consistent potential, respectively, while the semi-infinite self-energy matrices with complex eigenvalues. Starting from an initial guess for the device density matrix described in a suitable basis set, we calculate the self-consistent potential, which, added with the device Hamiltonian, generates the device Fock matrix. The Fock matrix, together with the contact self-energies, determines the nonequilibrium Green’s function that describes the causal response of the device to a unit excitation. The NEGF formalism gives us exact prescriptions thereafter for recomputing the nonequilibrium density matrix and current density, including the effects of many-body interactions and scattering within the device. The great advantage of this method is its generality: within the same framework, we can describe transport through various materials such as molecules, silicon transistors, nanowires, nanotubes, spintronic devices, and quantum dots.

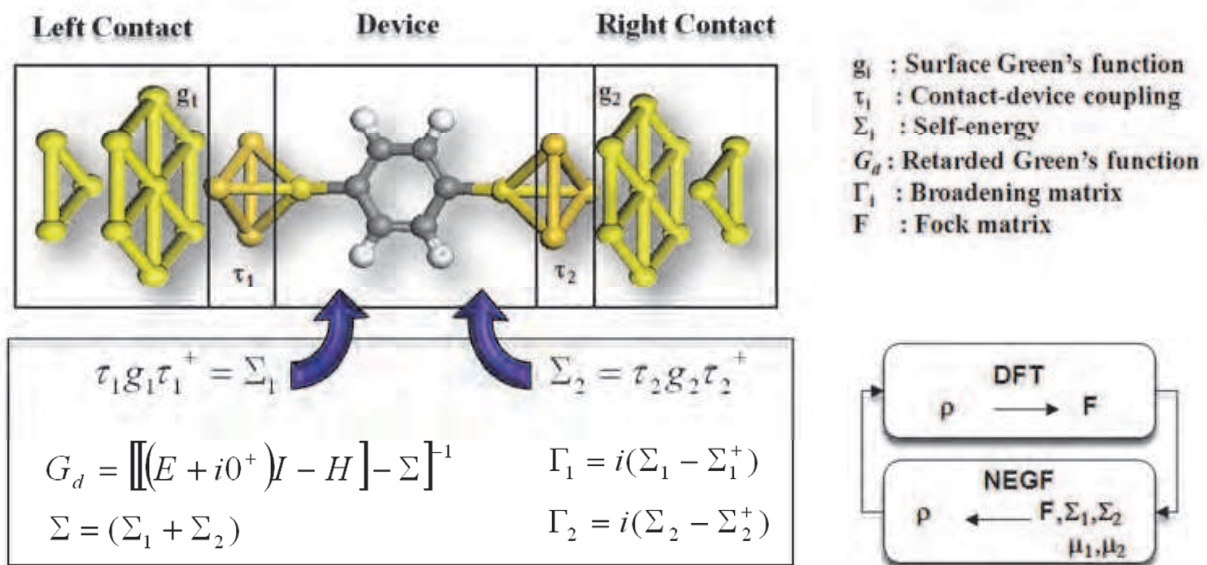


Fig. 2. Schematic of the nonequilibrium Green's function (NEGF) approach combined with density functional theory (DFT).

In the NEGF approach introduced above, the surface Green's functions describing semi-infinite electrodes attached to the defined device part from the left and right sides are derived using the Hamiltonian and overlap matrices corresponding to each CNT contact. The Green's function in this study is given by

$$G = (E^+ S - F - \Sigma_1 - \Sigma_2)^{-1} \tag{1}$$

Here E^+ denotes the energy plus an infinitesimal imaginary part (usually 10^{-5} or 10^{-6}), and S and F are the overlap and Fock matrices of the scattering part and $\Sigma_{1,2}$ is the self-energy matrix of the left and right electrode contacts, respectively. An applied bias leads to two different contact chemical potentials, $\mu_{1,2} = E_f \mp eV / 2$. The current through the scattering part is calculated by integrating the transmission coefficient within the bias window ($\mu_1 - \mu_2$) around the Fermi level.

$$I = (2e / h) \int_{-\infty}^{\infty} dE T(E, V) (f_1(E - \mu_1) - f_2(E - \mu_2)) \tag{2}$$

where the $f_{1,2}$ are the Fermi functions with electrochemical potential $\mu_{1,2}$

$$f_{1,2}(E) = \left(1 + \exp \left[\frac{E - \mu_{1,2}}{k_B T} \right] \right)^{-1} \tag{3}$$

$T(E)$ is the transmission coefficient between two electrodes derived from the Hamiltonian and the self-energies of electrodes:

$$T(E) = Tr \left[\Gamma_1 G \Gamma_2 G^+ \right] \tag{4}$$

3. Designing nanoelectronic diodes

3.1 Conventional diodes

In electronics, a diode is a two-terminal electronic component that conducts electric current in only one direction. The term usually refers to a semiconductor diode, the most common type today. The most common function of a diode is to allow an electric current to pass in one direction (called the diode's forward direction) while blocking current in the opposite direction (the reverse direction). A semiconductor diode's behavior in a circuit is given by its current-voltage characteristic, or I - V graph. The shape of the curve is determined by the transport of charge carriers through the so-called depletion layer or depletion region that exists at the p - n junction between differing semiconductors. When a p - n junction is first created, conduction band (mobile) electrons from the n -doped region diffuse into the p -doped region where there is a large population of holes (vacant places for electrons) with which the electrons "recombine". When a mobile electron recombines with a hole, both hole and electron vanish, leaving behind an immobile positively charged donor (dopant) on the n -side and negatively charged acceptor (dopant) on the p -side. The region around the p - n junction becomes depleted of charge carriers and thus behaves as an insulator.

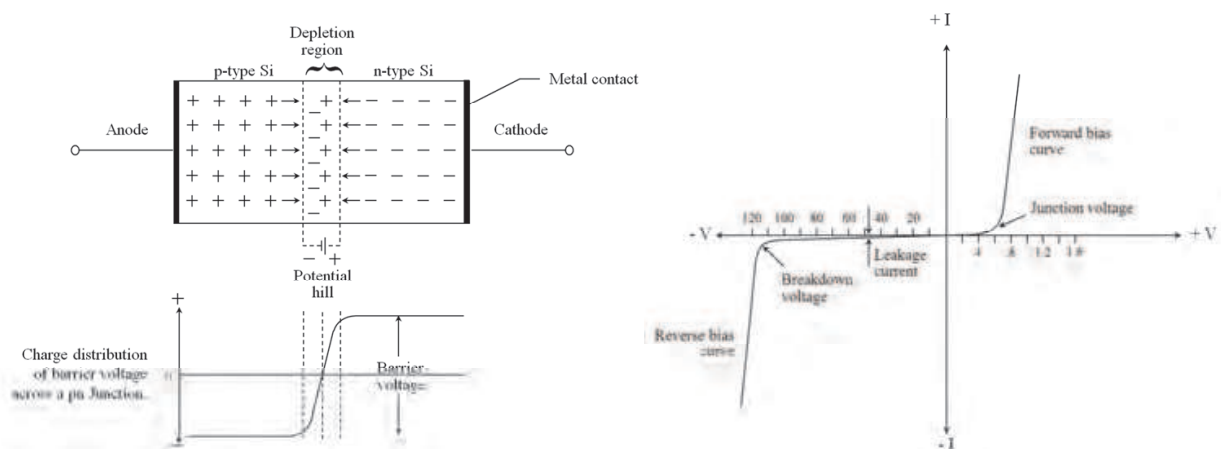


Fig. 3. p - n junction diode and I - V characteristics.

This unidirectional behavior is called rectification, and is used to convert alternating current to direct current, and to extract modulation from radio signals in radio receivers. However, diodes can have more complicated behavior than this simple on-off action. This is due to their complex non-linear electrical characteristics, which can be tailored by varying the construction of their p - n junction. These are exploited in special purpose diodes that perform many different functions. For example, specialized diodes are used to regulate voltage (Zener diodes), to generate radio frequency oscillations (Esaki diodes), to generate high speed response (Schottky diodes), to produce light (light emitting diodes (LED)), and to generate current (photodiode).

3.2 Designing strategy for nanoelectronic diodes

It has become clear through many studies that electron transport characteristics are influenced by the intrinsic properties of molecules, including their length, conformation, energy gap between the highest occupied molecular orbital (HOMO) and lowest unoccupied molecular orbital (LUMO), and the alignment of molecular levels relative to the

Fermi level of the contact. It has been demonstrated that the conductance of molecules can be controlled by the position of individual molecular levels. Therefore, the controlling the alignment of energy levels relative to the Fermi level of the contact allow us to design molecular scale devices using several building blocks such as carbon nanotubes.

Therefore, the strategy for designing nanoelectronic diodes is based on the control of the intrinsic properties, i.e. the electronic structure, of CNT by creating CNT junctions with organic linkages and chemical or physical doping. In this section, I will introduce four CNT junctions having Zener-, Schottky-, and Esaki-type diode characteristics.

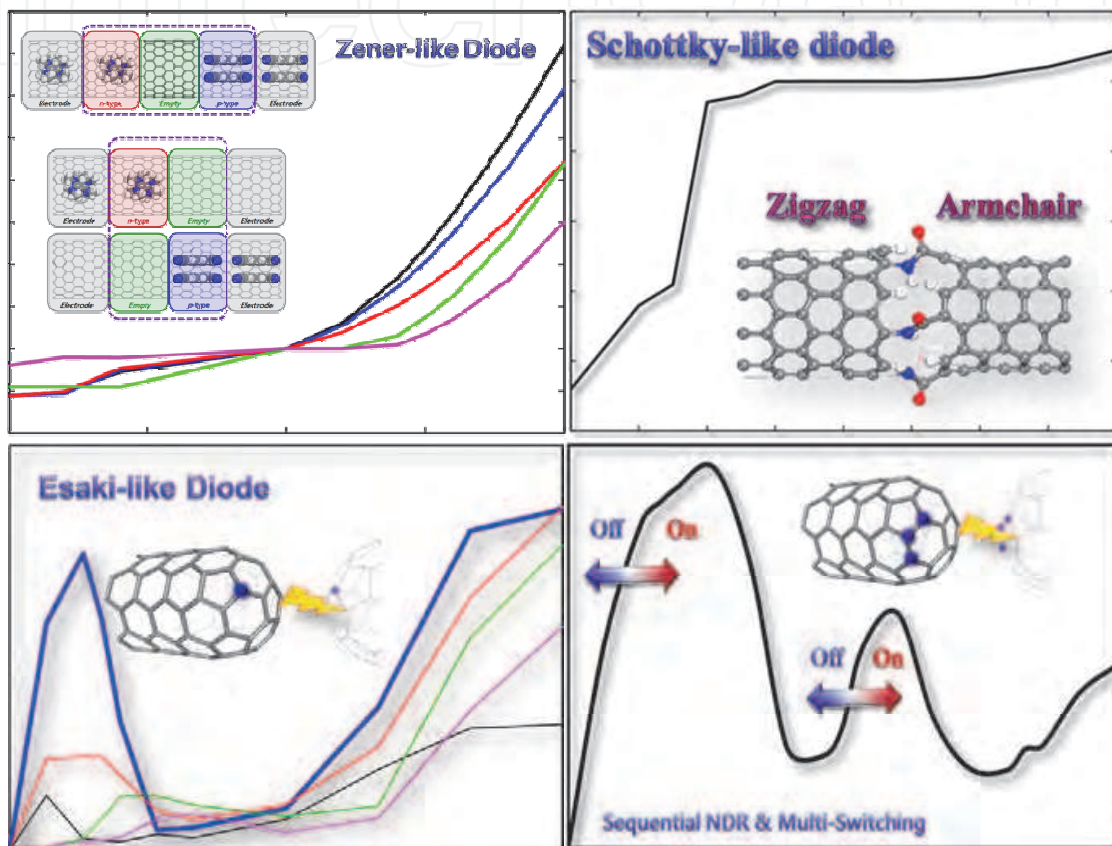


Fig. 4. Designed Zener-, Schottky-, and Esaki-type diodes.

3.3 Pure CNT

Detailed knowledge of the electron transport characteristics of pristine CNTs, both metallic (armchair) and semiconducting (zigzag) CNTs is a necessary requirement for investigating the designed CNT heterojunctions. Current-voltage ($I-V$) characteristics and bias dependence of the transmission curves, $T(E,V)$, of the pure CNTs are shown in Figure 5. $I-V$ curves and $T(E,V)$ plots show the intrinsic characteristics of each CNT with the white dotted lines indicating the bias window. The current is calculated by integrating the transmission coefficient within the bias window around the Fermi level. In fact, only the low-bias $I-V$ characteristics can be reasonably well reproduced by the equilibrium transmission characteristics, $T(E,V = 0)$. However, the deviation in both the magnitude and the peak position of transmission becomes significant at a large bias as can be seen from the shift of the peak near the Fermi level by the applied bias voltage. Hence, the evaluation of $T(E,V)$ is very important to reveal unique features of the systems investigated herein.

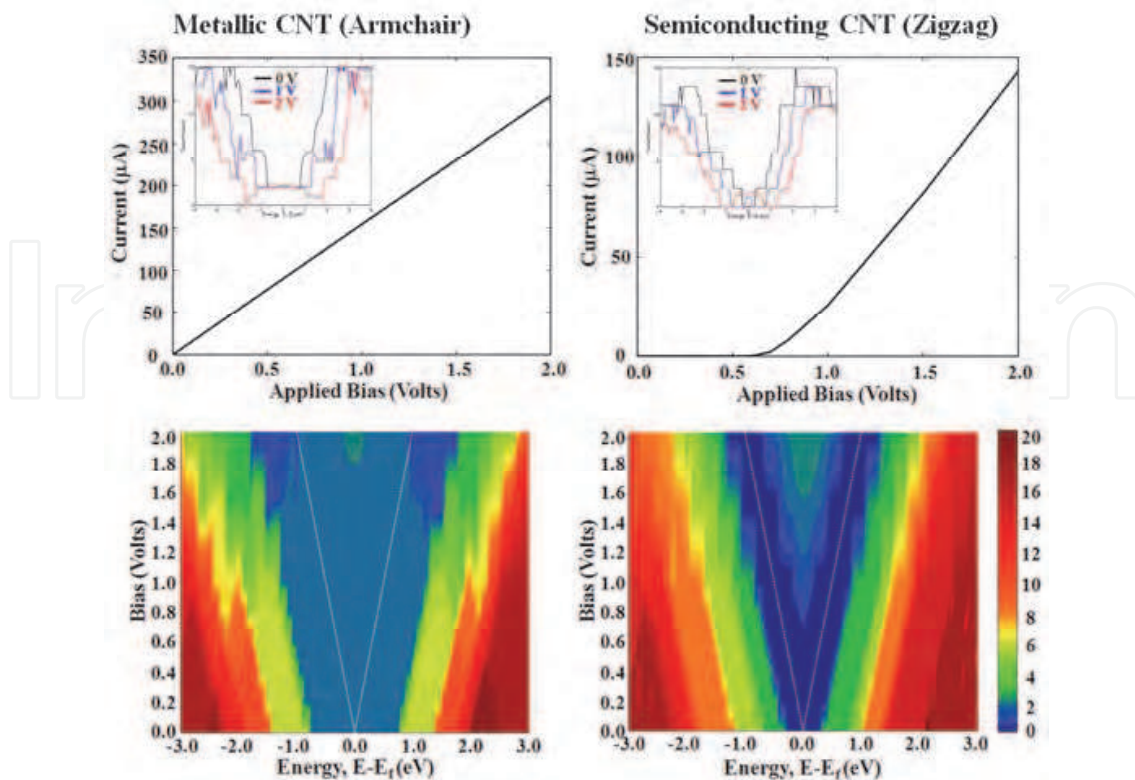


Fig. 5. $I-V$ curves and bias dependence of the transmission curves, $T(E, V)$, calculated at every 0.2 bias voltage for metallic and semiconducting pure carbon nanotube. $T(E, V)$ curves at 0.0, 1.0, and 2.0 V are shown in the inset. Dotted white lines indicate the range of current integration around the Fermi level.

The pure metallic CNT has two open conduction channels near the Fermi level at all applied bias ranges and shows a linear $I-V$ curve. On the other hand, the pure semiconducting CNT has a band-gap that increases according to the applied bias voltage near the Fermi level. However, when the applied bias voltage reaches a certain bias voltage, 0.8 V in this model, a new transmission peak appears near the Fermi level, which significantly contributes to the electron transport and current.

3.4 Zener-like diode: Organic molecules encapsulation & charge transfer

One-dimensional carbon nanotube (CNT) junctions can be designed by encapsulating p - and n -type organic molecules into CNTs with electrophilic tetracyano- p -quinodimethane (TCNQ) and nucleophilic tetrakis(dimethylamino)ethylene (TDAE) molecules, where the charge transfer play an important role in determining the electron transport characteristics and lead to materials with unique properties, p - n junction diode, *i.e.* Zener-like diode.

The operational device characteristics of organic molecules encapsulated CNT junctions originate from distinct response of intrinsic transmission peaks of pure CNTs and the distinctive response is determined by the manner of the charge transfer. The charge transfer between CNT and doped organic molecules causes lateral shift of the transmission peaks, and the charge transfer between the encapsulated organic molecules cause vertical shift of the transmission peaks. Therefore, by controlling the charge transfer, *i.e.* the electron affinity (EA) and ionization potential (IP) of the encapsulated molecules, we can finely tune the operational device characteristics.

3.4.1 Modeling

Each tetracyano-p-quinodimethane (TCNQ) and nucleophilic tetrakis(dimethylamino) ethylene (TDAE) molecules molecule is encapsulated in carbon nanotubes (13,0) and (17,0) (CNT13 and CNT17), as shown in Figure 6. Encapsulated organic molecules are separated by 4.342 Å or 4.480 Å for TCNQ and 5.675 Å for TDAE at periodic boundary condition with 12.780 Å of z-axis cell size. In the case of TCNQ molecule, we considered parallel(P) and tilted(T) stacking patterns at CNT17 due to a large diameter. So, we denote the designed models as "CNTa-b_c", where "a", "b", and "c" respectively mean the size of zigzag CNT, encapsulated organic molecule, and stacking pattern.

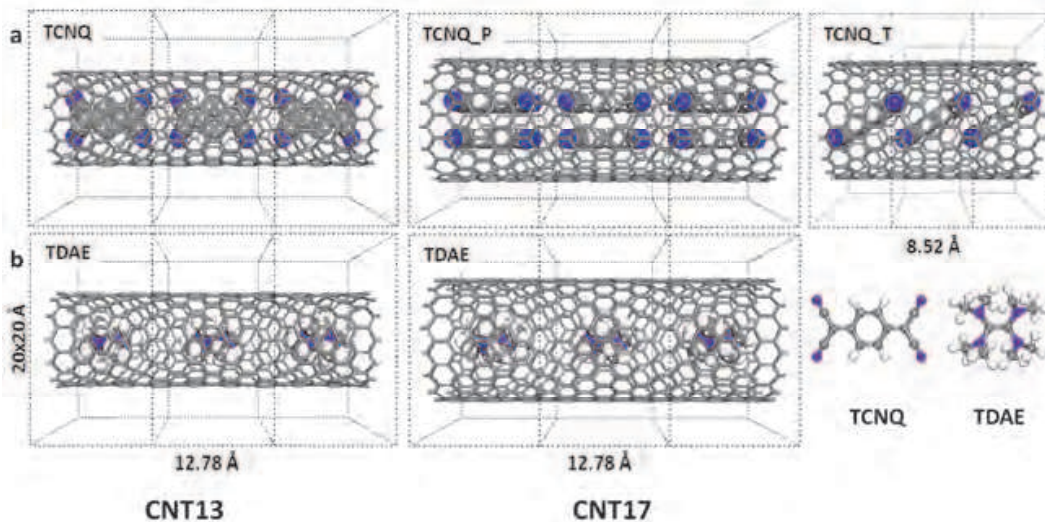


Fig. 6. Schematic of (a) TCNQ or (b) TDAE encapsulated carbon nanotubes (13,0) and (17,0) (CNT13 and CNT17). In the case of TCNQ molecule, parallel(P) and tilted(T) stacking patterns are considered at CNT17.

3.4.2 Electron transport characteristics of TCNQ and TDAE encapsulated CNTs

When we encapsulate TCNQ and TDAE molecules into the semiconducting CNTs, the charge transfer between organic molecule and CNT affects the band structures of CNT. But the change of band structures is opposite each other because TCNQ and TDAE have different electrostatic features, electrophilic and nucleophilic. The electronic band structures of TCNQ and TDAE encapsulated CNT17s, pure CNT17 and organic molecules are shown in Figure 7.

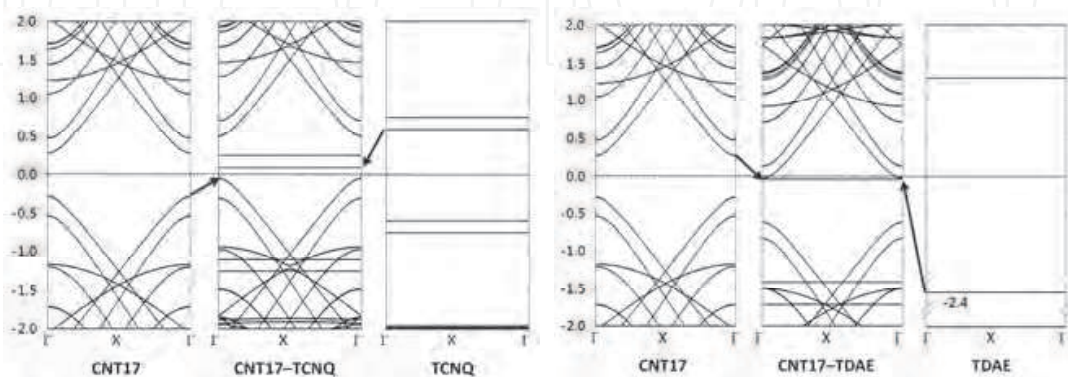


Fig. 7. Electronic band structures of TCNQ and TDAE encapsulated CNT17s, and pure CNT17 and organic molecules (TCNQ and TDAE).

The flat bands near the Fermi level are derived from the lowest unoccupied molecular orbital (LUMO) states of TCNQ, and the highest occupied molecular orbital (HOMO) states of TDAE, where each LUMO and HOMO creates acceptor and donor states in the gap of CNT. The band structures shift up and down by doping of TCNQ and TDAE, respectively. The band in CNT17-TDAE closely lies in the top of the CNT valence band, which induces charge transfer from CNT to TCNQ. The higher-lying band in CNT17-TDAE, however, overlaps with the bottom of the CNT conduction band. The bands are partially filled, indicative of effective electron transfer from TDAE to CNT. It is seen that the relatively large change of HOMO level in TDAE is derived from the large charge transfer, that is the doping effect of *n*-type encapsulated organic molecule is more significant than that of *p*-type one.

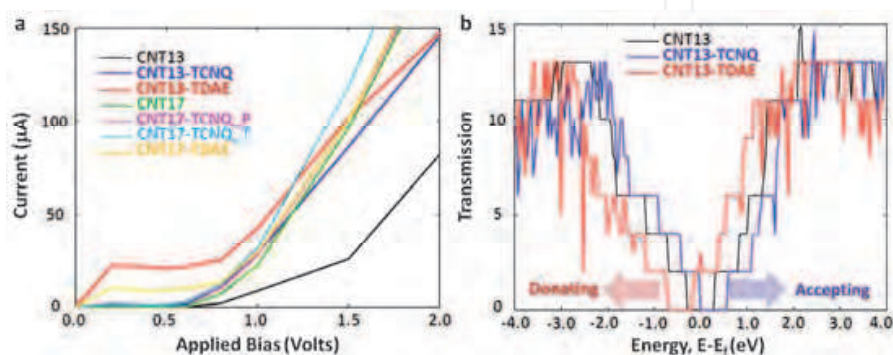


Fig. 8. (a) I - V curves and (b) the transmission curves, $T(E, V=0)$, of TCNQ or TDAE encapsulated CNTs, "CNTa-b_c", where "a", "b", and "c" respectively mean the size of zigzag CNT, encapsulated organic molecule, and stacking pattern.

Let us now discuss the electron transport characteristics of *p*- and *n*-type doped CNTs. Current-voltage (I - V) and equilibrium transmission, $T(E, V = 0)$, and bias dependence of the transmission curves, $T(E, V)$, of TCNQ and TDAE encapsulated CNTs are compared to the pure CNT13 and CNT17 as shown in Figure 8. The pure semiconducting CNTs (CNT13 and CNT17) have a band-gap that increases according to the applied bias voltage near the Fermi level. So, pure semiconducting CNTs do not have current under low bias voltage. However, when the applied bias voltage reaches a certain voltage (~ 0.6 V), a new transmission peak appears near the Fermi level, which significantly contributes to the electron transport and current as shown in Figure 8.

TCNQ encapsulated CNTs show similar current behavior with pure semiconducting CNTs regardless of parallel or tilted conformation. There is almost no current until 0.6 V, beyond which the current starts to increase. In contrast TCNQ encapsulated CNTs, the change of energy level is larger for TDAE encapsulated CNTs and the direction of shift of transmission peak is opposite, moreover transmission peak crosses over the Fermi level and enters into the bias window as seen in Figure 8(b). Therefore, TDAE encapsulated CNTs have very small currents when applied bias is smaller than a critical bias voltage (~ 0.8 V), above which the current begins to increase owing to a new transmission peak within the bias window. Furthermore, this new transmission peak increases with increasing applied bias. It is seen that the I - V characteristic of TDAE encapsulated CNTs show varistor-like behavior (i.e., a resistor with a significantly nonohmic current-voltage characteristic) because the amplitude and number of conducting channels, which are located in the integration window, are constant for a large range of applied voltages (from ~ 0.0 to ~ 0.8 V) The varistors are often used to protect circuits against excessive voltage.

Accordingly, it is worth mentioning that the effect of non-covalent doping essentially originates from the shift of the transmission peaks. The charge transfer between CNT and doped organic molecules causes lateral shift of the transmission peaks, shift left or shift right, which gives different behavior under the applied bias voltages. And the shift can be controlled by tuning the electron affinity (EA) and ionization potential (IP) of the encapsulated molecules.

3.4.3 Electron transport characteristics of p-n junctions with TCNQ and TDAE encapsulated CNTs

We have investigated the operational device characteristics of the organic molecules encapsulated CNT *p-n* junctions, as shown in Figure 9. We incorporated empty region between *n*-type CNT17-TDAE and *p*-type CNT17-TCNQ with the distance of “*d*”, in order to reduce direct interaction between doped organic molecules (Junction 1-3). In addition, we considered CNT *p-n* junctions composed of only one type of CNT, *p*- or *n*-type, and pure semiconducting CNT (CNT17) (Junction4 and 5), where CNT17 acts as both an electron acceptor and electron donor according to the dopant of counterpart. Scattering region and electrode are defined as shown in Figure 9.

Figure 10 shows the *I-V* characteristics of the organic molecules encapsulated CNT *p-n* junctions, where all designed junctions display completely non-linear and asymmetric *I-V* curves and provide rectifying behaviors regardless of the type of junction with a large current under forward bias while almost no current under reverse bias, resembling that of a conventional Zener diode. The current rises for a positive bias applied to the left electrode. The rectifying behavior can be understood by the induced electric field between the left *n*-

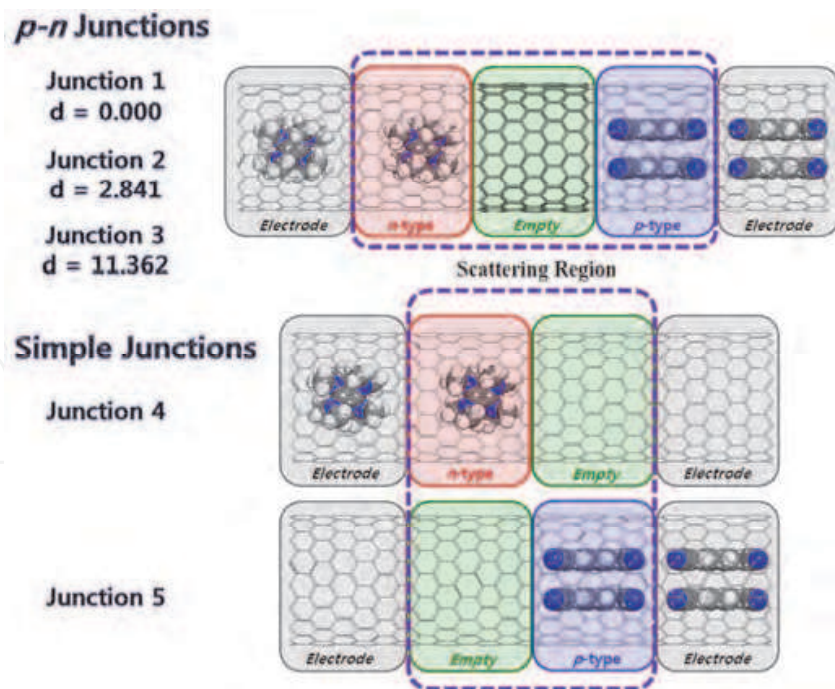


Fig. 9. Schematic of the TDAE and TCNQ encapsulated *p-n* junctions. Junction1, Junction2 and Junction3 contain *n*-type TDAE and *p*-type TCNQ molecules, and empty region is inserted between them with the cell size of “*d*”. Junction4 and Junction5 have only *n*-type TDAE or *p*-type TCNQ respectively. Scattering regions are denoted by dotted box.

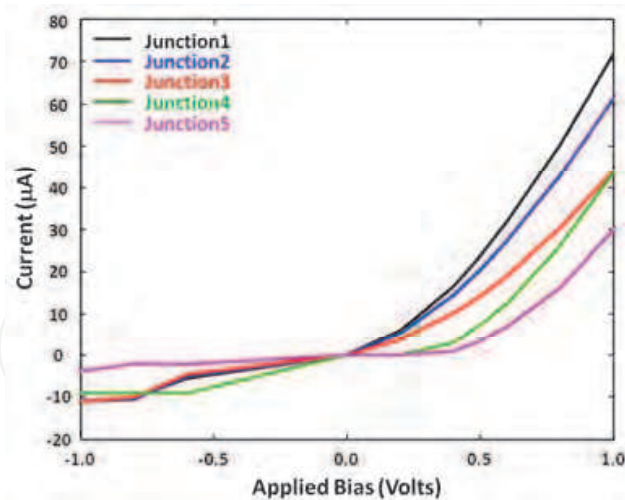


Fig. 10. I - V characteristics of TDAE and TCNQ encapsulated CNT p - n junctions

type CNT17-TDAE to the right p -type CNT17-TCNQ. Because the encapsulated TCNQ and TDAE molecules are electrophilic and nucleophilic, electric field is induced by charge transfer between them, and the direction is from the left n -type CNT17-TDAE to p -type CNT17-TCNQ. If the direction of the electric field is the same to the direction of the electron flow under a forward, it has current. But, under reverse bias (negative bias), the electric field acts as a potential barrier of the electron flow. Therefore, the rectifying behavior is determined by the orientation of the electric field arising from the charge transfer between p - and n -type doped CNTs. Furthermore, the difference of rectifying ability among the designed junctions implies the role of the charge transfer and induced electric field.

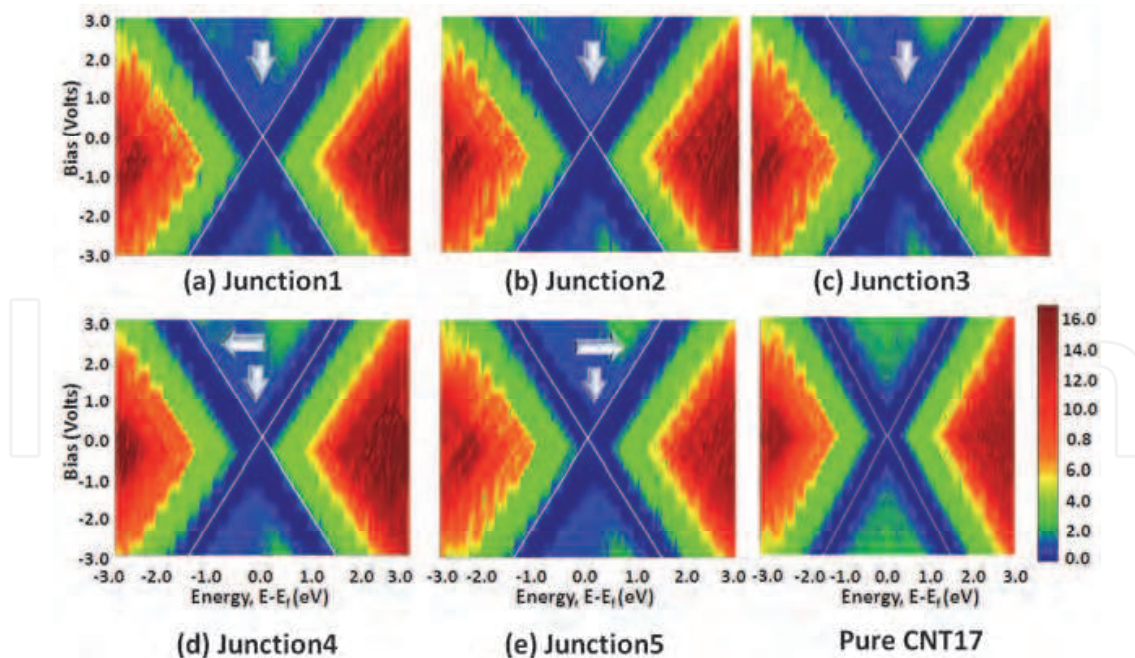


Fig. 11. Bias dependence of the transmission curves, $T(E,V)$, calculated at every 0.2 bias voltage for the TDAE and TCNQ encapsulated CNT p - n junctions compared to that of pure CNT17: (a) Junction1, (b) Junction2, (c) Junction3, (d) Junction4, and (e) Junction5. White arrows point out the shift of transmission peaks compared to that of pure CNT17. White lines indicate the range of current integration around the Fermi level.

Junction1-3 show the decrease of current with increasing the size of empty region under forward bias (positive bias), and Junction4 and 5 have smaller current because the large empty region or absence of one type of dopant molecule suppresses a charge transfer between *p*- and *n*-type CNTs.

In previous section, we have mentioned that lateral shift of the transmission peaks is seen for the TDAE or TCNQ encapsulated CNTs according to the dopants. In contrast, vertical shift of the transmission peaks is also seen the organic molecules encapsulated *p-n* junctions by charge transfer between encapsulated *n*-type and *p*-type molecules, as seen in Figure 11. The designed CNT *p-n* junctions show significant shift of the transmission peaks to negative bias region, i.e. shift down, as indicated by white arrow, in comparison to the symmetric behavior of pure CNT17, which leads the designed CNT *p-n* junctions to have rectifying behavior. Weak rectifying behavior and weak current of Junction4 and 5 can be explained by weak vertical shift of the transmission peaks, furthermore, the inherent effect of organic molecule encapsulation, lateral shift of transmission peaks, is seen, because they have only one type of dopant molecules. So, we can address that the rectifying behavior originate from asymmetric vertical shift of the transmission peaks, and which induced by the charge transfer between the encapsulated organic molecules, TDAE and TCNQ. And the shift also can be controlled by tuning EA and IP of the encapsulated molecules.

It is concluded, that the effect of non-covalent doping and the rectifying behavior essentially originates from the shift of the transmission peaks through charge transfer between the CNT and different types of dopants. Therefore, we can realize conventional Zener-like diode using the organic molecule encapsulated CNT junctions.

3.5 Schottky-like diode: Organic linkage & dipole moment

One-dimensional carbon nanotube (CNT) junctions with peptide linkages can be designed, where the incorporation of peptide linkages and their associated dipole moments play an important role in determining the electron transport characteristics and lead to materials with unique properties, such as Schottky-like behavior.

The incorporation of peptide linkages gives rise to the suppression of current and the effects are more significant for metallic CNTs than for semiconducting CNTs. Furthermore, the electron transport characteristics of the designed junctions depend on the direction of the dipole moment associated to the peptide linkages, which brings about asymmetric I-V behavior.

3.5.1 Modeling

The carbon nanotube models used in this study are metallic (armchair (5,5)) and semiconducting (zigzag (10,0)) CNTs. The intramolecular heterojunctions are assembled with two CNT units and five peptide linkages, shown in Figure 12. When less than five covalent linkages are employed or the chemical bridges are asymmetrically distributed around the CNT mouths, the conformational flexibility of the resulting model junctions increases considerably.

Figure 12 shows the investigated intramolecular heterojunctions composed of metallic and semiconducting CNTs, and peptide linkage. SM1 and SM2 indicate semiconductor/metal, and metal/semiconductor junctions with peptide linkages, respectively. The SM1 and SM2 junctions are distinguished by the asymmetric peptide linkage composed of C=O and N-H bonds. In the SM1 junction, the C=O and N-H bonds are, correspondingly, connected to the metallic and semiconducting CNTs and vice versa in the SM2 junction.

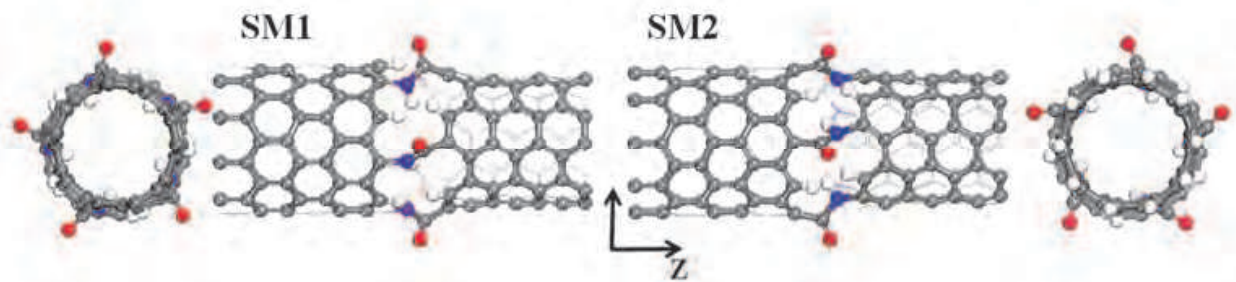


Fig. 12. Optimized structures of four carbon nanotube intramolecular heterojunctions with peptide linkages, SM1, and SM2.

3.5.2 Electron transport characteristics

Figure 13 shows the I - V characteristics of intramolecular heterojunctions, SM1, and SM2. The directions of their dipole moments are oriented from the C=O bond to the N-H bond. Therefore, the direction of the dipole moment can be either the same or opposite with respect to the direction of the applied bias; each positive and negative applied bias correspondingly gives parallel or anti-parallel alignment with the direction of the dipole moment vector.

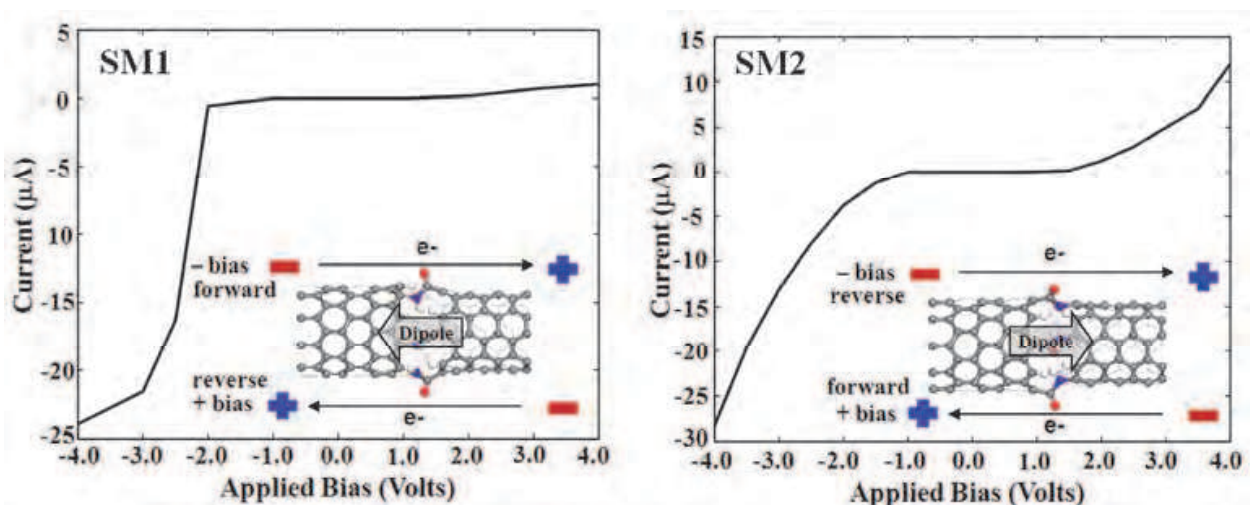


Fig. 13. I - V curves of four carbon nanotube intramolecular heterojunctions, SM1, and SM2. The directions of forward and reverse bias, electron flow, and dipole moment are indicated in the inset.

Junctions made by CNTs with different chiralities evoke unique properties and multiple functionalities. Indeed, the metal and semiconductor junction with a positive barrier height has a pronounced rectifying behavior, as in a typical Schottky diode. The difference in the electronic structures and screening properties of metallic and semiconducting CNTs gives rise to different band-bending profiles and, subsequently, a Schottky barrier at the junction interface, which explains the rectifying behavior across the junction. A large current exists under forward bias, while almost no current exists under reverse bias. In Figure 13, the SM1 junction displays a completely non-linear and asymmetric I - V curve, resembling that of a Schottky diode. The current rises sharply above a threshold voltage, -2.0 V, for a negative

bias applied to the left semiconducting CNT. There is a small increase in current for reverse bias.

The difference between the SM1 and SM2 junctions results from the connecting way between peptide linkages and CNT electrodes. In other words, the orientation of the dipole moment arising from the peptide linkages plays an important role in the resulting Schottky-like behavior. In the SM1 junction, the C=O and N-H bonds are correspondingly connected to the metallic and semiconducting CNTs, respectively, which sets up the direction of the dipole moment vector from the metallic CNT to the semiconducting CNT. Therefore, the charge transfer is induced from the semiconducting CNT to the metallic CNT, where the direction of the charge transfer is the same to the direction of the electron flow under a forward bias of the Schottky diode. It means that the SM1 junction resembles an *n*-type Schottky diode. In contrast, the SM2 junction resembles the p-type one. Accordingly, it can be explained why Schottky-like behavior is observed in our SM1 junction but not in the SM2 junction. In addition, the large dipole moment associated to the SM2 junction (7.21 Debye) also intensifies the symmetric *I*-*V* characteristics because a reverse bias is aligned parallel to the dipole moment vector, resulting in an increase of current. Under a reverse bias, the change of current is much larger in the SM2 junction than in the SM1 junction, as seen in Figure 13.

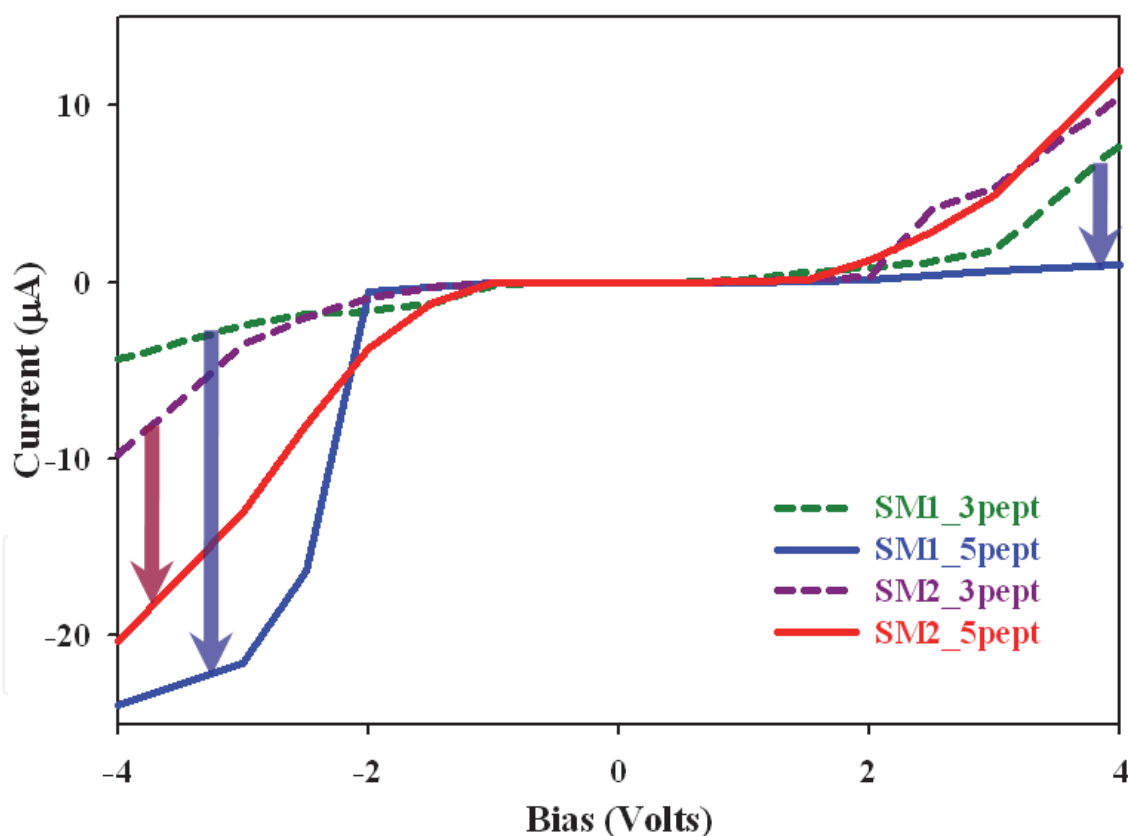


Fig. 14. *I*-*V* curves of SM1 and SM2 junctions at the different number of peptide linkages.

We have investigated the effects of the number of peptide linkage on the electron transport characteristics of the SM1 and SM2 junctions to clarify the effect of the dipole moment to the Schottky barrier and rectifying behavior. In Figure 14, it is seen that the tunneling current of the SM1 junction is suppressed at the reverse biases (positive biases) by increasing the number of peptide linkages, which reveals the dependence of the Schottky barrier on the

dipole moment. In contrast, there is no significant dipole dependence at the SM2 junction. The increase of the tunneling current of both the SM1 and SM2 junctions at the negative biases originates from the increase of tunneling channels when the number of linkages increases from three to five peptides.

Based on these results, we can prove that the Schotkky barrier is basically induced by the intrinsic nature of the pure semiconducting-metallic CNT junctions; afterwards the induced Schotkky barrier can be controlled at the SM1 junction by varying the dipole moment through the number of incorporated peptide linkages, whereas the effect of the dipole moment is not significant at the SM2 junction.

3.6 Esaki-like diode / multi-switching: Chemical doping & donor state

One-dimensional carbon nanotube (CNT) junctions with two single- (or multi-)nitrogen-doped (N-doped) capped carbon nanotubes (CNTs) facing one another can be designed, where the modification of the molecular orbitals by the N-dopants generates a conducting channel in the designed CNT junctions, inducing a negative differential resistance (NDR) behavior, which is a characteristic feature of the Esaki-like diode, that is, tunneling diode. And by controlling doping level, NDR based multi-switching behaviour can be achieved.

The NDR behavior significantly depends on the N-doping site and the facing conformations of the N-doped capped CNT junctions. Furthermore, a clear interpretation is presented for the NDR behavior by a rigid shift model of the HOMO- and LUMO-filtered energy levels in the left and right electrodes under the applied biases.

3.6.1 Modeling

The front end of the N-doped capped CNT(5,5) and CNT(9,0) is closed with a hemisphere of fullerene and the carbon atoms on the other end are passivated with hydrogen atoms. Then nitrogen atom is substituted at the cap or sidewall region as denoted by letters in Figure 15(a). In order to provide the device part of the two-probe system (contact-device-contact), that is, N-doped capped CNT junctions, saturated hydrogen atoms are detached from the optimized N-doped capped CNT(5,5) and CNT(9,0) and the modified structure is replicated so as to face one another with the proper distance, as shown in Figure 15(a). The distances between two facing N-doped capped CNTs are referred to as the distance of the fullerene dimer because the designed CNTs have a hemisphere of fullerene as a cap. Then the left and right sides of the CNT junctions are connected to appropriate semi-infinite CNT electrodes with the same chiralities of the CNT junctions.

In the single-N-doped capped CNT junctions, we consider four different conformations depending on the chirality of the CNTs (armchair(5,5) and zigzag(9,0)) and the spatial arrangement of the nitrogen atoms in the designed CNT junctions. Because of the distinct cap structures of the armchair(5,5) and zigzag(9,0) CNTs, pentagon- and hexagon-facing conformations are possible for the CNT(5,5) and CNT(9,0), respectively. In addition, both pentagon- and hexagon-facing conformations have the eclipsed and staggered conformations owing to the spatial arrangement of the N-dopants.

In addition, the designed multi-N-doped capped CNT junctions are considered, which are b-site_multi-N-doped CNT junctions according to the number of doped nitrogen atoms and their conformations compared to that of single-N-doped capped CNT(5,5) junction, **55b**. In

the multi-N-doped capped CNT junctions, only eclipsed arrangement of armchair(5,5) CNT junctions are considered. Whole designed geometries are depicted in the Figure 15(b).

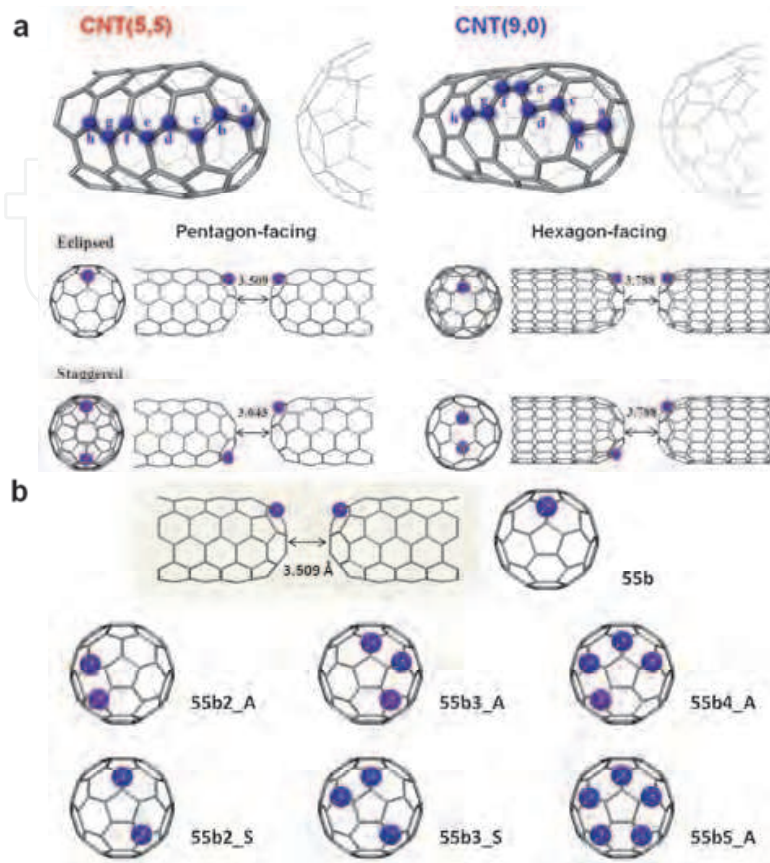


Fig. 15. (a) Schematic of the two facing single-N-doped capped carbon nanotubes (CNTs) in different conformations according to the chirality of the CNTs (armchair(5,5) and zigzag(9,0)) and the spatial arrangement of the nitrogen dopants; pentagon- or hexagon-facing and eclipsed or staggered conformations. The notations of **55xE** and **90xS** mean that **x** is nitrogen doping site and **E** and **S** mean eclipsed and staggered. The letters (**a - h**) indicate the atomic sites for replacing carbon with nitrogen atoms. (b) Schematic of the two facing multi-N-doped capped carbon nanotubes according to the number of doped nitrogen atoms and their conformations compared to that of single-N-doped capped CNT(5,5) junction, **55b**. Models of have nitrogen atoms at only "b" doping site (b-site_multi-N-doped CNTs).

3.6.2 Electron transport characteristics

Current-voltage (I - V) characteristics of the single-N-doped capped CNT(5,5) and CNT (9,0) junctions at the eclipsed and staggered conformations, respectively, are compared to the pure capped CNT junction as shown in Figure 16. The **55xE** and **90xS** notations mean that **x** is the single-N-doping site and **E** and **S** are eclipsed and staggered, respectively. The remarkable feature emerging from the I - V characteristics of the N-doped CNT junctions is that the tunneling current between two single-N-doped capped CNTs is dramatically increased by N-doping and a negative differential resistance (NDR) is observed. The NDR is a typical feature of the Esaki-like diode, that is, tunneling diode. In the eclipsed conformation of the single-N-doped capped CNT(5,5) junctions, a sharp current peak appears at an applied bias range of $0.0V < V < 0.8 V$, while the current is very low around the $1.0V < V < 1.5V$ applied bias range.

Furthermore, it is seen that the height of the sharp current peak (I_{peak}) and the peak position (V_{peak}) strongly depend on the N-doping site. The V_{peak} gradually moves up to higher bias range when the doping site is changed from cap to sidewall: **55aE** is 0.2, **55bE** is 0.4, **55cE** is 0.5, **55dE** is 0.8, **55eE** is 0.8, and **55fE** is 1.0 V. And the **55bE** junction has a maximum I_{peak} value, 11.73 μA , which is considerably larger as compared to that of other junctions. In addition, the **55bE** junction has the largest peak-to-valley ratio (PVR), 15.03. The PVR value of the **55bE** junction is more than twice the PVR value of the typical solid-state Esaki-diode, that is, GaAs/AlGaAs diode. In contrast to the dependence on the N-doping site, there is no significant difference of the I - V characteristics between two eclipsed and staggered conformations. Both conformations show that the NDR behavior and the current peak and PVR value depend on the single-N-doping site in the same way. Such features of the I - V characteristics are also seen in the single-N-doped capped CNT(9,0) junctions, however the tunnelling current is significantly suppressed as compared to that of the single-N-doped capped CNT(5,5) junctions. This reveals that electron transport characteristics strongly depend on the facing conformation induced by the chirality of the CNT without regard for the eclipsed or staggered conformations. The pentagon-facing conformation of CNT(5,5) junctions provides a large tunnelling current as compared to the hexagon-facing conformation of CNT(9,0). In addition, it is found that the observed NDR behavior is strongly dependent on the N-doping site.

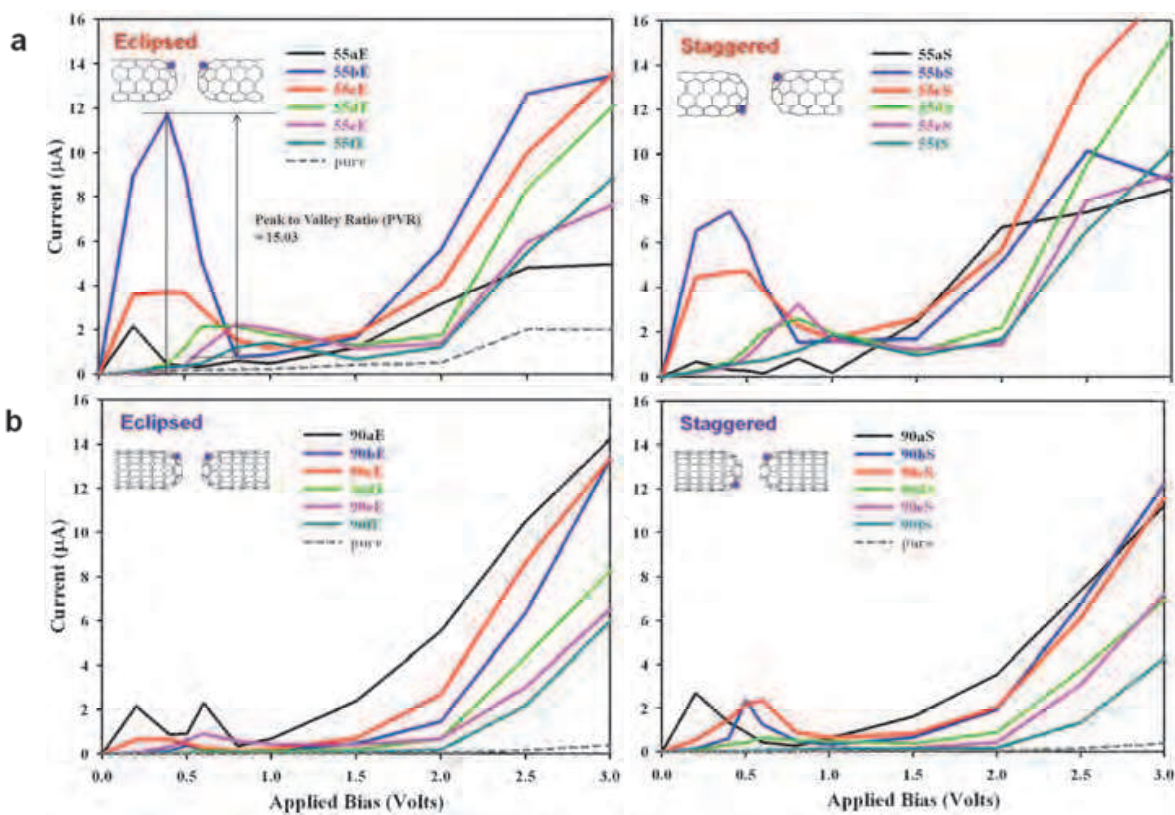


Fig. 16. a) I - V curves of the N-doped capped (a) CNT(5,5) and (b) CNT(9,0) junctions in the eclipsed and staggered conformations, respectively, as compared to the pure capped CNT junctions. The nitrogen atom is substituted at the **a**, **b**, **c**, **d**, **e**, and **f** doping sites, which are denoted by **55(90)a**, **55(90)b**, **55(90)c**, **55(90)d**, **55(90)e**, and **55(90)f**. The structures of junction PVRs are shown in the inset.

Therefore, we have increased the number of doped nitrogen atoms at **b** site, b-site_multi-N-doped CNT(5,5) junctions, in order to investigate how NDR behavior response the number of doped nitrogen atoms. I - V characteristics of the multi-N-doped capped CNT junctions are compared to that of the single-N-doped CNT(5,5), **55b**, and pure CNT(5,5) junctions, as shown in Figure 17.

The remarkable feature emerging from the I - V characteristics is that the tunneling current is dramatically increased by nitrogen doping and a negative differential resistance (NDR) is observed compared to that of pure CNT(5,5) junction. In comparison of the I - V characteristics of the multi-N-doped CNT junctions to that of **55b** junction, it is seen that the NDR behavior is conserved or reinforced, and the tunneling current is enhanced by addition of nitrogen atoms. The trend is strong for b-site_multi-N-doped CNT junctions rather than for multi-site_multi-N-doped CNT junctions. But the tendency is not so for all junctions, because the NDR behavior disappears at **55b3_S** and **55b5_A** junctions. And it is seen the conformational dependency, in which the junctions having aggregated conformation have enhanced current, while separated conformation gives suppressed current. The difference is clearly seen at **55b2** and **55b3** junctions, where the aggregated conformation (**55b2_A** and **55b3_A**) reinforces the current and NDR behavior, while separated conformation (**55b2_S** and **55b3_S**) suppresses the current and NDR behaviour.

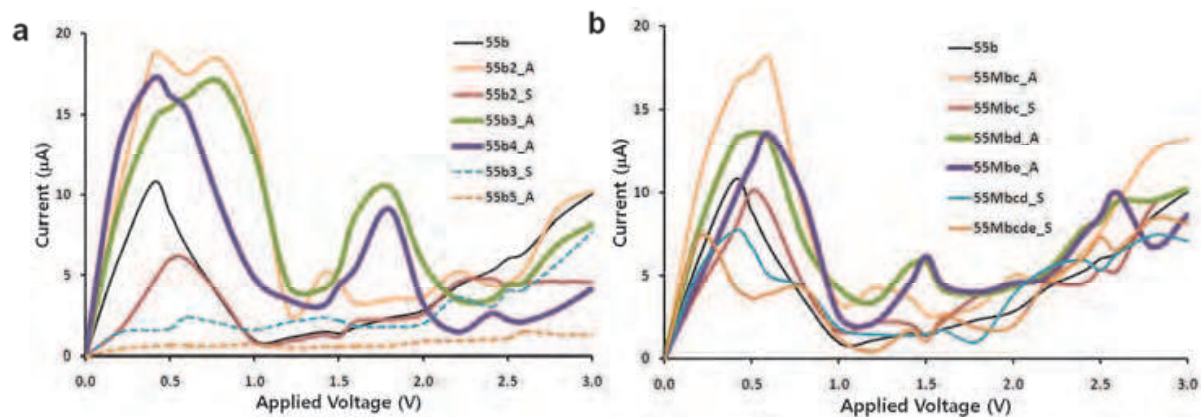


Fig. 17. (a) I - V curves of the multi-N-doped capped CNT(5,5) junctions compared to those of the single-N-doped capped CNT(5,5), and **55b**.

The I - V curve shows relatively large peak-to-valley ratio (PVR), > 4 , although the height of the sharp current peak and the peak position (V_{peak}) depend on designed junctions. The remarkable feature emerging from the results is sequential NDR behavior is induced by additional nitrogen atoms and the feature depends on the conformation, aggregated or separated. In b-site_multi-N-doped CNT junctions, **55b2_A**, **55b3_A** and **55b4_A** junctions of aggregated conformation, have another new sharp current peak at $1.5 \text{ V} < V < 2.0 \text{ V}$ applied bias range (V_{peak2}) and current valley at $2.0 \text{ V} < V < 2.5 \text{ V}$ applied bias range (V_{valley2}). Beside, in the case of multi-site_multi-N-doped CNT junctions, weak new current peak is seen for **55b2_A**, **55Mbd_A**, and **55Mbe_A**. Among the multi-N-doped capped CNT junctions, **55b3_A** and **55b4_A** junctions provide clear sequential NDR behavior. The observed sequential NDR behavior can be used for successive switching process in which each switching occurs at different times when the bias current is gradually increased as describe in Figure 18.

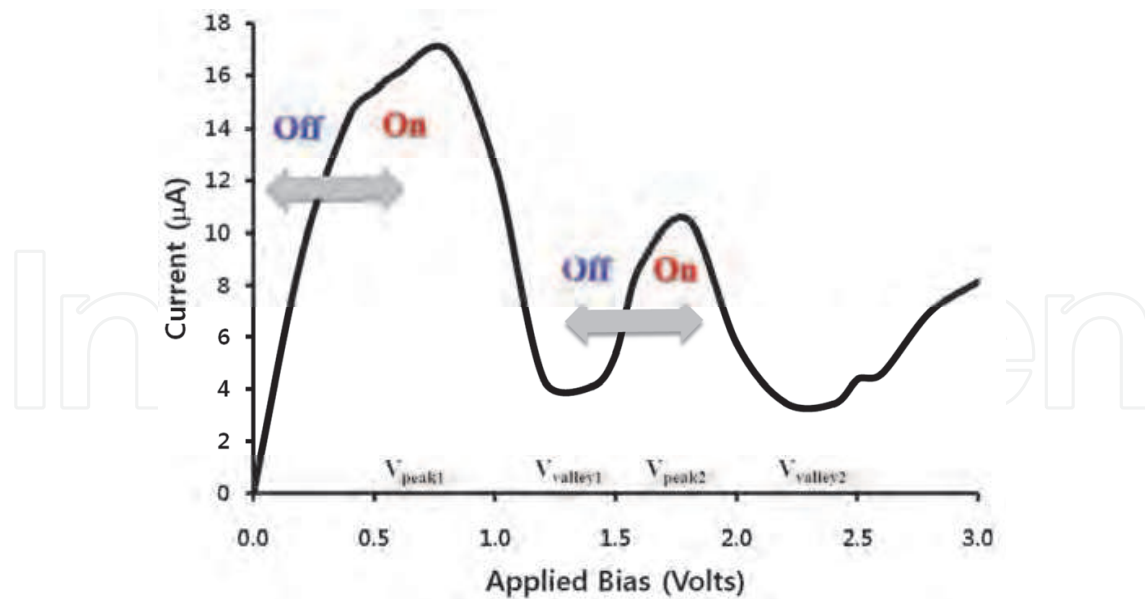


Fig. 18. Multi-switching behavior of the multi-N-doped capped CNT(5,5) junction, 55b3_A.

3.6.3 The role of the nitrogen dopants for the NDR behavior

Such distinguishable electron transport characteristics usually originate from the intrinsic nature of the molecule, such as the molecular energy level alignment with respect to the Fermi level and their response to the applied bias voltage. In this work, a new option is the doping of CNTs with nitrogen atoms, which tailors the electronic structure of the nanotube. Nitrogen has a profound effect on the structural arrangement and electronic properties of the CNTs, such as a strong donor state near the Fermi level. It has been shown theoretically that a small amount of dopant can drastically modify the electronic transport properties of the tube. For zigzag semiconducting CNTs, doping with a single nitrogen impurity increases current flow, whereas doped metallic CNTs with boron or nitrogen atoms produce quasibound impurity states of a definite parity and reduces the conductance via resonant backscattering. Although we designed 1D heterojunctions with two N-doped capped CNTs compared to the use of open-ended CNTs previously reported, the N-dopants correspondingly affect the electron transport characteristics of the N-doped capped CNT junctions, which are enhancement of tunneling current and appearance of NDR behavior through new conducting channels.

So, in advance we have investigated the molecular orbitals of one side of the designed junctions. If the molecular orbitals are well delocalized and contribute to the cap region, they can facilitate electron conduction between the linked CNTs. In Figure 19, it can be seen that the doped nitrogen atom enhances the contribution of the molecular orbitals at the cap region, especially the majority-spin HOMO-1 and minority-spin HOMO. In addition, the majority-spin LUMO and LUMO+1, and minority-spin LUMO+1 and LUMO+2 orbitals expand into the sidewall region from the cap region. Accordingly, in the N-doped capped CNT(5,5), two groups of energy levels (HOMOs and LUMOs) generate the HOMO filtered energy levels (HFEL) and the LUMO filtered energy levels (LFEL) through coupling with the semi-infinite CNT electrode. However, when the nitrogen is doped at the sidewall region (*f* doping site) instead at the cap region (*b* doping site), the enhancement on the cap region is weak, which is revealed as a low tunneling current and small I_{peak} value.

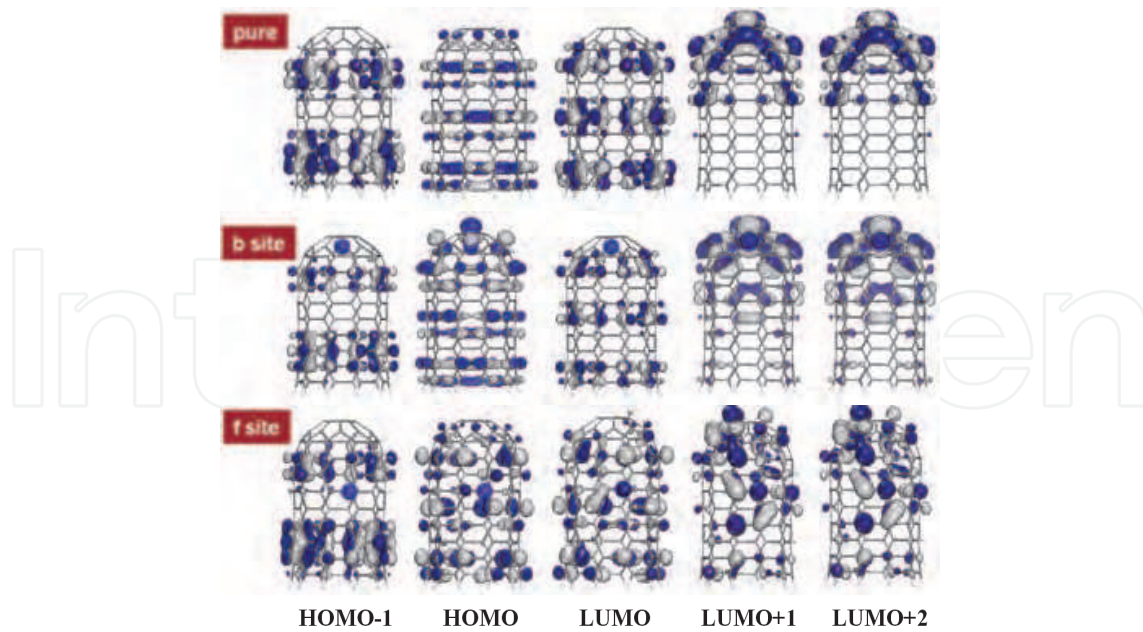


Fig. 19. Molecular orbitals of the pure and N-doped capped CNT(5,5) **b** and **f** doping sites.

Therefore, the NDR behavior in the N-doped capped CNT junctions can be interpreted by a rigid shift model of the LFEL and HFEL in the left and right electrodes under the applied biases (Figure 20). Under the applied biases, the alignment between LFEL and HFEL of each electrode gradually increases until V_{peak} due to the fact that the applied bias leads to two different contact chemical potentials. When the applied bias reaches V_{peak} , HFEL and LFEL of each electrode are well-aligned and a peak appears in the I - V curve. At V_{valley} , the tunneling current becomes low because of mismatching between the HFEL and LFEL of each electrode. However, at the higher bias voltage, the alignment between the LFEL (HFEL) and CFEL (VFEL) (conduction and valence filtered energy levels, respectively) of each electrode takes place again and the tunneling current increases.

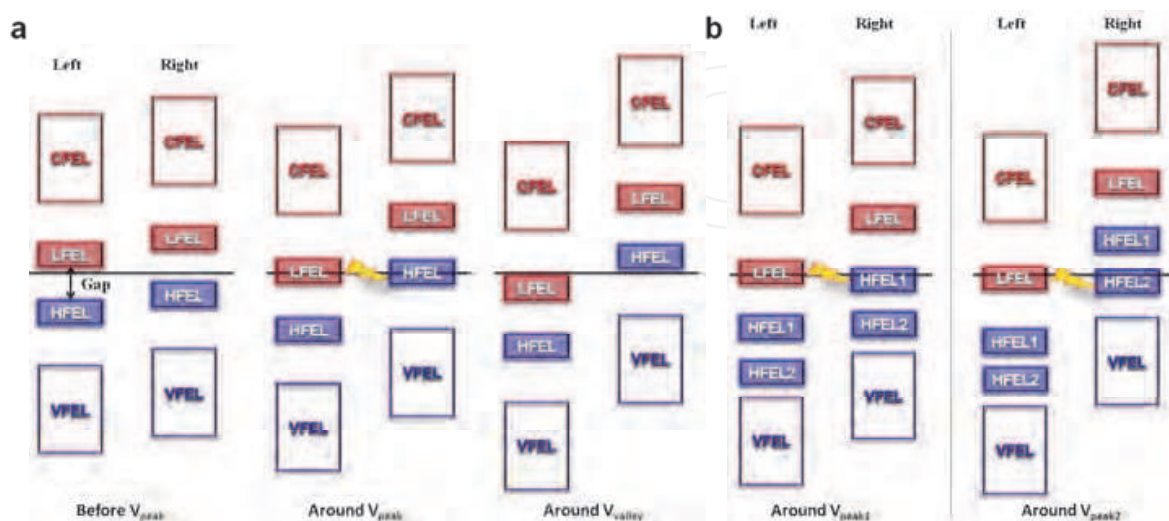


Fig. 20. Diagram of the relative shift of the energy levels in the left and right (a) single- and (b) multi-N-doped capped CNTs under applied biases around V_{peak} .

It is concluded, that the doped nitrogen atom plays an important role in the electron transport characteristics of the designed CNT junctions by modifying their molecular orbitals so as to have the NDR behavior. Therefore, we can realize conventional Esaki-like diode using the N-doped capped CNT junctions.

4. Conclusion

It has been shown how we can design nanoelectronic component embodied with interesting device characteristics, especially rectifying diodes. Simple strategy for designing nanoelectronic diodes is creating carbon nanotube (CNT) junction and controlling their electronic structure. Several types of one-dimensional CNT junctions can be designed by organic linkages and chemical or physical doping. Each designed CNT junction show unique electron transport characteristics, Zener-, Schottky-, and Esaki-like diode.

The charge transfer between CNT and encapsulated organic molecules causes lateral shift of the transmission peaks, and the charge transfer between the encapsulated organic molecules cause vertical shift of the transmission peaks. Therefore, by controlling the charge transfer, *i.e.* the electron affinity (EA) and ionization potential (IP) of the encapsulated molecules, we can finely tune the operational device characteristics.

We could know that the tunneling barrier can be controlled by the strength of dipole moment. Therefore, the rectifying behavior of Schottky-like diode can be obtained by incorporating the peptide linkages to the metallic/semiconducting CNT junctions, where the direction of the dipole moment plays an important role in the determination of the rectifying behavior.

Finally, we showed that the doped nitrogen atoms modify the molecular orbitals so as to generate a conducting channel in the designed CNT junctions by inducing a negative differential resistance (NDR) behavior, which is a characteristic feature of the Esaki-like diode, *i.e.* tunneling diode. And by controlling doping level, NDR based multi-switching behaviour can be achieved.

It is concluded that the designed CNT junctions open the door to the design of nanoelectronic components embodied with interesting device characteristics. We believe that the results will give an insight into the design and implementation of various electronic logic functions based on CNTs for applications in the field of nanoelectronics.

5. Acknowledgment

The authors sincerely thank the crew of the Center for Computational Materials Science of the Institute of Materials Research, Tohoku University, for their continuous support of supercomputing facilities. The authors are very thankful for the support of the CREST headed by Prof. Motoko Kotani.

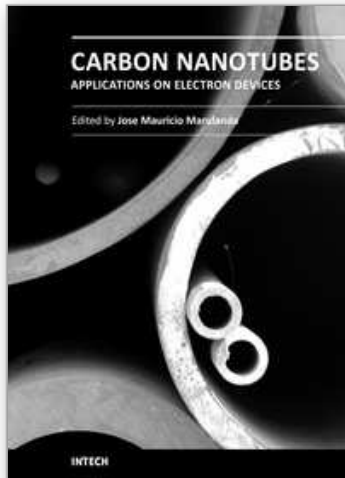
6. References

- Aviram, A.; Ratner, M.A. (1974). *Chemical Physics Letters*, Vol. 29, No.2, (November 1974), pp.277-283, ISSN 0009-2614
- Dekker, C. (1999). *Physics Today*, Vol.52, (May 1999), pp.22-28, ISSN 0031-9228
- Misewich, J. A.; Martel, R.; Avouris, Ph.; Tsang, J. C.; Heinze, S.; Tersoff, J. (2000). *Science*, Vol.300, No.2, (May 2000), pp.783-786, ISSN 0036-8075

- Joachim, C.; Gimzewski, J. K.; Aviram, A. (2000). *Nature*, Vol.408, No.30, (November 2000), pp.541-548, ISSN 0028-0836
- Tseng, G. Y.; Ellenbogen, J.C. (2001). *Science*, Vol.294, No.9, (November 2001), pp.1293-129, ISSN 0036-8075
- Kwok, K. S.; Ellenbogen, J. C. (2002). *Materials Today*, Vol.5, No.2, (February 2002), pp.28-37, ISSN 1369-7021
- Lee, S. U.; Belosludov, R. V.; Mizuseki, H.; Kawazoe, Y. (2011). *Nanoscale*, Vol.3, No.4, (April 2011), pp.1773-1779, ISSN 0306-0012
- Brandbyge, M.; Mozos, J. L.; Ordejón, P.; Taylor, J.; Stokbro, K. (2002). *Physical Review B*, Vol.65, No.16, (March 2002), pp.165401-17, ISSN 1098-0121
- Mozos, J. L.; Ordejón, P.; Brandbyge, M.; Taylor, J.; Stokbro, K. (2002). *Nanotechnology*, Vol.13, No.3, (March 2002), pp.346-351, ISSN 1550-7033
- Avouris, Ph. (2002). *Account of Chemical Research*, Vol.35, No.12, (July 2002), pp.1026-1034, ISSN 1520-4898
- Takenobu, T.; Takano, T.; Shiraishi, M.; Murakami, Y.; Ata, M.; Kataura, H.; Achiba, Y.; Iwasa, Y. (2003). *Nature Materials*, Vol.2, (October 2003), pp.683-688, ISSN 1476-1122
- Zhou, O.; Shimoda, H.; Gao, B.; Oh, S.; Fleming, L.; Yue, G. (2002). *Account of Chemical Research*, Vol.35, No.12, (November 2002), pp.1043-1053, ISSN 1520-4898
- Liu, Y.; Guo, H. (2004). *Physical Review B*, Vol.69, No.11, (March 2004), pp.115401-6, ISSN 1098-0121
- Son, Y. W.; Ihm, J.; Cohen, M. L.; Louie, S. G.; Choi, H. J. (2005). *Physical Review Letters*, Vol. 95, No.21, (November 2005), pp.216602-4, ISSN 0031-9007
- García-Suárez, V. M.; Ferrer, J.; Lambert, C. L. (2006). *Physical Review Letters*, Vol. 96, No.10, (March 2006), pp.106804-4, ISSN 0031-9007
- Chen, Z., Appenzeller, J.; Lin, Y.-M.; Sippel-Oakley, J.; Rinzler, A. G.; Tang, J.; Wind, S.; Solomon, P.; Avouris, Ph. (2006). *Science*, Vol.311, No.24, (March 2006), pp.1735, ISSN 0036-8075
- Zhu, W.; Kaxiras, E. (2006). *Nano Letters*, Vol.6, No.7, (June 2006), pp.1425-1419, ISSN 1530-6984
- Balzani, V.; Credi, A.; Venturi, M. (2007). *Nano Today*, Vol.2, No.2, (April 2007), pp.18-25, ISSN 1748-0132;
- Pichler, T. (2007). *Nature Materials*, Vol.6, (May 2007), pp.332-333, ISSN 1476-1122
- Khazaei, M.; Lee, S. U.; Pichierri, F.; Kawazoe, Y. (2007). *Journal of Physical Chemistry C*, Vol.111, No.33, (August 2007), pp.12175-12180
- Lee, S. U.; Belosludov, R. V.; Mizuseki, H.; Kawazoe, Y. (2007). *Journal of Physical Chemistry C*, Vol.111, No.42, (October 2007), pp.15397-15403, ISSN 1542-3050
- Sumpter, B. G.; Meunier, V.; Herrera, J. M. R.; Silva, E. C.; Cullen, D. A.; Terrones, H.; Smith, D. J.; Terrones, M. (2007). *ACS Nano*, Vol.1, No.4, (November 2007), pp.369-375, ISSN 1936-0851
- Mizuseki, H.; Belosludov, R. V.; Uehara, T.; Lee, S. U.; Kawazoe, Y. (2008). *Journal of Korean Physical Society*, Vol.52, No.4, (April 2008), pp.1197-1201, ISSN 1976-8524
- Khazaei, M.; Lee, S. U.; Pichierri, F.; Kawazoe, Y. (2008). *ACS Nano*, Vol.2, No.5, (May 2008), pp.939-943, ISSN 1936-0851
- Lee, S. U.; Belosludov, R. V.; Mizuseki, H.; Kawazoe, Y. (2008). *Small*, Vol.4, No.7, (July 2008), pp.962-969, ISSN 1613-6829

- Lee, S. U.; Khazaei, M.; Pichierri, F.; Kawazoe, Y. (2008). *Physical Chemistry Chemical Physics*, Vol.10, No.34, (July 2008), pp.5225-5231, ISSN 1463-9076
- Lee, S. U.; Belosludov, R. V.; Mizuseki, H.; Kawazoe, Y. (2009). *Small*, Vol.5, No.15, (April 2009), pp.1769-1775, ISSN 1613-6829
- Lee, S. U.; Mizuseki, H.; Kawazoe, Y. (2010). *Physical Chemistry Chemical Physics*, Vol.12, No.37, (June 2010), pp.11763-11769, ISSN 1463-9076
- Lee, S. U.; Mizuseki, H.; Kawazoe, Y. (2010). *Nanoscale*, Vol.2, No.12, (July 2010), pp.2758-2764, ISSN 0306-0012
- Lee, S. U.; Belosludov, R. V.; Mizuseki, H.; Kawazoe, Y. (2011). *Nanoscale*, Vol.3, No.4, (Feb 2011), pp. 1773-1779, ISSN 0306-0012

IntechOpen



Carbon Nanotubes Applications on Electron Devices

Edited by Prof. Jose Mauricio Marulanda

ISBN 978-953-307-496-2

Hard cover, 556 pages

Publisher InTech

Published online 01, August, 2011

Published in print edition August, 2011

Carbon nanotubes (CNTs), discovered in 1991, have been a subject of intensive research for a wide range of applications. In the past decades, although carbon nanotubes have undergone massive research, considering the success of silicon, it has, nonetheless, been difficult to appreciate the potential influence of carbon nanotubes in current technology. The main objective of this book is therefore to give a wide variety of possible applications of carbon nanotubes in many industries related to electron device technology. This should allow the user to better appreciate the potential of these innovating nanometer sized materials. Readers of this book should have a good background on electron devices and semiconductor device physics as this book presents excellent results on possible device applications of carbon nanotubes. This book begins with an analysis on fabrication techniques, followed by a study on current models, and it presents a significant amount of work on different devices and applications available to current technology.

How to reference

In order to correctly reference this scholarly work, feel free to copy and paste the following:

Sang Uck Lee and Yoshiyuki Kawazoe (2011). Nanodesign and Simulation Toward Nanoelectronic Devices, Carbon Nanotubes Applications on Electron Devices, Prof. Jose Mauricio Marulanda (Ed.), ISBN: 978-953-307-496-2, InTech, Available from: <http://www.intechopen.com/books/carbon-nanotubes-applications-on-electron-devices/nanodesign-and-simulation-toward-nanoelectronic-devices>

INTECH
open science | open minds

InTech Europe

University Campus STeP Ri
Slavka Krautzeka 83/A
51000 Rijeka, Croatia
Phone: +385 (51) 770 447
Fax: +385 (51) 686 166
www.intechopen.com

InTech China

Unit 405, Office Block, Hotel Equatorial Shanghai
No.65, Yan An Road (West), Shanghai, 200040, China
中国上海市延安西路65号上海国际贵都大饭店办公楼405单元
Phone: +86-21-62489820
Fax: +86-21-62489821

© 2011 The Author(s). Licensee IntechOpen. This chapter is distributed under the terms of the [Creative Commons Attribution-NonCommercial-ShareAlike-3.0 License](#), which permits use, distribution and reproduction for non-commercial purposes, provided the original is properly cited and derivative works building on this content are distributed under the same license.

IntechOpen

IntechOpen